Pflügers Archiv - European Journal of Physiology (2023) 475:1009–1024
https://doi.org/10.1007/s00424-023-02834-8

SENSORY PHYSIOLOGY

# Contribution of TRPC3-mediated $Ca^{2+}$ entry to taste transduction

**Alexander P. Cherkashin[1] · Olga A. Rogachevskaja[1] · Alexander A. Khokhlov[1] · Natalia V. Kabanova[1] · Marina F. Bystrova[1] · Stanislav S. Kolesnikov[1]**

Received: 6 March 2023 / Revised: 19 May 2023 / Accepted: 22 June 2023 / Published online: 27 June 2023
© The Author(s), under exclusive licence to Springer-Verlag GmbH Germany, part of Springer Nature 2023

## Abstract

The current concept of taste transduction implicates the TASR/PLCβ2/$IP_3$R3/TRPM5 axis in mediating chemo-electrical coupling in taste cells of the type II. While generation of $IP_3$ has been verified as an obligatory step, DAG appears to be a byproduct of $PIP_2$ cleavage by PLCβ2. Here, we provide evidence that DAG-signaling could play a significant and not yet recognized role in taste transduction. In particular, we found that DAG-gated channels are functional in type II cells but not in type I and type III cells. The DAG-gated current presumably constitutes a fraction of the generator current triggered by taste stimulation in type II cells. Bitter stimuli and DAG analogs produced $Ca^{2+}$ transients in type II cells, which were greatly decreased at low bath $Ca^{2+}$, indicating their dependence on $Ca^{2+}$ influx. Among DAG-gated channels, transcripts solely for TRPC3 were detected in the taste tissue, thus implicating this channel in mediating DAG-regulated $Ca^{2+}$ entry. Release of the afferent neurotransmitter ATP from CV papillae was monitored online by using the luciferin/luciferase method and Ussing-like chamber. It was shown that ATP secretion initiated by bitter stimuli and DAG analogs strongly depended on mucosal $Ca^{2+}$. Based on the overall findings, we speculate that in taste transduction, $IP_3$-driven $Ca^{2+}$ release is transient and mainly responsible for rapid activation of $Ca^{2+}$-gated TRPM5 channels, thus forming the initial phase of receptor potential. DAG-regulated $Ca^{2+}$ entry through apically situated TRPC3 channels extends the primary $Ca^{2+}$ signal and preserves TRPM5 activity, providing a needful prolongation of the receptor potential.

**Keywords** Taste transduction · Taste cells · $Ca^{2+}$ entry · TRPC3 · DAG · ATP release

## Introduction

The taste bud, a functional unit of the periphery taste system, is a heterogeneous self-renewing population of 50–80 cells of different morphological, functional, and molecular features. Taste cells of three morphotypes, type I to type III, have been identified and shown to be distinct functionally and by molecular features [61, 65]. While taste cells of the type II and type III are electrically excitable, unexcitable type I cells presumably perform a glia-like function and create chemical and physical barriers within a taste bud by wrapping type II and III cells [61, 72]. The type II group includes three major functionally separate cell subpopulations, each expressing dedicated G-protein-coupled receptors (GPCRs) to detect sweet, umami, or bitter compounds [2]. The TAS1R family comprises three members, which form two heterodimeric receptors, one for certain L-amino acids and nucleotides (TAS1R1/TAS1R3) and another for natural and artificial sweeteners (TAS1R2/TAS1R3) [48, 49]. Evidence, however, exists that sweet and umami transduction can also involve TAS1R-independent mechanisms [61, 65]. Bitter taste is mediated by multiple GPCRs from the TAS2R family [1, 14]. Type III cells are responsible for sour taste, and among multiple proposed candidates, recent findings favor the $H^+$-selective channel otopetrin1 to be a most likely sour sensor [36, 68]. Reportedly, the type III cellular group also contains subsets of cells responsive either to carbonation [15] or to salts at high concentrations [33, 53] or even to bitter, sweet, and umami stimuli [4].

The recent study of salt responsivity of fungiform taste bud cells revealed type II-like cells being responsive to NaCl with $Ca^{2+}$ mobilization in amiloride-insensitive

✉ Stanislav S. Kolesnikov
staskolesnikov@yahoo.com

[1] Institute of Cell Biophysics, Pushchino Scientific Center for Biological Research of the Russian Academy of Sciences, 3 Institutskaya Street, Pushchino, Moscow Region 142290, Russia

manner, thus being high-salt sensors [57]. In addition, the fungiform taste bud contains previously non-recognized cells of two types, excitable and non-excitable, both expressing epithelial $Na^+$ channels as molecular sensors for sodium taste [51]. In excitable cells, amiloride-sensitive $Na^+$ influx evokes action potentials not accompanied by $Ca^{2+}$ signaling. These cells presumably mediate sodium taste, as they communicate with an afferent taste nerve via CALHM1/3 ion channels previously shown to serve as a release conduit for ATP, an afferent neurotransmitter in type II cells [41, 59]. It thus appears that taste transduction in a particular taste papilla may involve a specific set of chemosensory cells.

Although sweet, umami, and bitter receptors are segregated into distinct cell lines, taste transduction in specified cells is associated with a rather similar sequence of intracellular events from binding of sapid molecules to taste GPCRs to action potential (AP) firing [61, 65]. The tastant-induced signaling downstream of TAS1/TAS2 receptors invariably involves activation of phospholipase Cβ2 (PLCβ2), the generation of inositol 1,4,5-trisphosphate ($IP_3$), and $Ca^{2+}$ release from $Ca^{2+}$ store through $IP_3$ receptors of the type 3 ($IP_3R3$). The associated $Ca^{2+}$ transient stimulates $Ca^{2+}$-gated cation channels TRPM5 and presumably TRPM4 to generate depolarizing receptor potential and to initiate an AP train driving ATP release. This canonical concept is based on a body of strong evidence, including the genetic knock-out of key signaling proteins, such as PLCβ2, $IP_3R3$, TRPM5, and CALHM1, which caused significant impact on taste responses assayed on the behavioral, neuronal, and cellular levels [5, 27, 66, 74].

Interestingly, pheromone-induced GPCR signaling in sensory neurons in the vomeronasal organ (VNO) also involves PLC-mediated cleavages of phosphatidylinositol 4,5-bisphosphate ($PIP_2$) into soluble $IP_3$ and membrane-bound diacylglycerol (DAG). Existing evidence involves DAG signaling rather than $IP_3$-mediated $Ca^{2+}$ release in mediating pheromone transduction [63]. In particular, evidence exists that the DAG-gated channel TRPC2 mediates pheromone-induced receptor potential in VNO neurons [39]. In contrast, a role of DAG signaling in physiology of taste cells remains elusive: among currently available reports, to our knowledge, only one implicates DAG-gated TRPC3 in fat transduction in cells operating in mouse fungiform taste buds [45].

In this study, we assayed mouse taste cells isolated mostly from the circumvallate (CV) papilla and found that DAG-gated $Ca^{2+}$ permeable channels, presumably TRPC3, are functionally expressed in type II cells. Our overall findings suggest that DAG-regulated $Ca^{2+}$ influx through TRPC3 could markedly contribute to intracellular $Ca^{2+}$ signals, which are normally triggered by tastants in order to generate the TRPM5-meduated receptor potential. Therefore, it appears that DAG signaling is an essential factor of taste transduction in taste cells of the type II.

## Materials and methods

### Isolation of taste cells

All experimental protocols were in accordance with local regulatory requirements and the European Communities Council Directive (2010/63/EU) and approved by the Commission on Biosafety and Bioethics (Institute of Cell Biophysics–Pushchino Scientific Center for Biological Research of the Russian Academy of Sciences, Permission no. 4/062020 (June 12, 2020)). Mice (C57Bl6) of 2–4 months old, and both sexes were used in experiments. Taste cells and taste buds were harvested from circumvallate (CV) and foliate papillae as described previously [6]. In summary, mice were sacrificed using carbon dioxide and cervical dislocation. After removal, a tongue was injected between the epithelium and muscle layers with 1.0 mg/ml collagenase B, 1.8 mg/ml dispase II, 0.4 mg/ml elastase, and 0.5 mg/ml trypsin inhibitor (all from Sigma-Aldrich, St. Louis, MO, USA) dissolved in a solution (mM): 120 NaCl, 20 KCl, 1 $MgCl_2$, 1 $CaCl_2$, 10 glucose, and 20 HEPES-NaOH (pH 7.8). Once injected, the tongue was incubated in the oxygenated Ca-free solution (in mM): 130 NaCl, 10 KCl, 0.7 $CaCl_2$, 1.1 $MgCl_2$, 1 EGTA, 1 EDTA, 10 HEPES-NaOH (pH 7.4), and 10 glucose, for 30–35 min. After the treatment, a lingual epithelium was peeled off from the underlying muscle, pinned serosal side up in a dish covered with Sylgard resin, and then incubated in the Ca-free solution for 10–30 min. The isolated epithelium was kept at room temperature in a solution (in mM: 130 NaCl, 5 KCl, 1 $MgCl_2$, 2 $CaCl_2$, 10 HEPES-NaOH (pH 7.4), 10 glucose, 5 Na-pyruvate) for 4–6 hrs. To obtain individual taste buds, those were removed from the CV papilla by gentle suction using a fire-polished pipette with an opening of 80–100 µm. Taste cells were isolated by using suction pipettes with tips of 50–70 µm. The obtained cellular material was then expelled into an electrophysiological or photometric chamber.

### Electrophysiology

Ion currents were recorded, filtered, and analyzed using an Axopatch 200 B amplifier, Digidata 1440A and MiniDigi 1B interfaces, and pClamp 10 software (all from Molecular Devices, LLC., San Jose, CA, USA). External solutions were delivered by a gravity-driven perfusion system at a rate of 0.1 ml/sec. Cells were polarized either by serial voltage pulses of appropriate duration at a 10 mV step or by voltage ramp (1 mV/ms). Generally, the perforated patch approach was used with recording pipettes containing (mM):

140 CsCl, 1 $MgCl_2$, 0.5 EGTA, 10 HEPES-CsOH (pH 7.2), and 400 µg/ml Amphotericin B. The basic bath solution included (mM) 140 NaCl, 5 KCl, 2 $CaCl_2$, 1 $MgCl_2$, 10 HEPES-NaOH (pH 7.4), and 5 glucose. When necessary, 2 mM $CaCl_2$ was replaced with 2 µM $CaCl_2$ or with 0.5 mM EGTA + 0.4 mM $CaCl_2$. In the last case, free $Ca^{2+}$ was reduced to ~260 nM at 23°C according to calculations with Maxchelator program (http://maxchelator.stanford.edu). The recording chamber of nearly 75 µl has been described previously [30].

## $Ca^{2+}$ imaging

Isolated taste buds or cells were plated onto a photometric chamber (~150 µl), which represented a disposable coverslip (Menzel-Glaser, Thermo Fisher Scientific) with an attached ellipsoidal resin wall. The chamber bottom was coated with Cell-Tak (Corning, NY, USA) enabling strong cell adhesion. Once attached to the bottom, a taste cell preparation was incubated in the bath solution containing Fluo-8AM (4 µM) (AAT Bioquest, Sunnyvale, CA, USA) and Pluronic (0.02%) (Molecular Probes, Waltham, MA, USA) at room temperature (RT) (23–25°C). Given that quick rundown was characteristic of taste responses of isolated taste cells and taste buds, they were loaded for 15 min and 25 min, respectively, rinsed with the bath solution for several times and immediately assayed.

Experiments were carried out using an inverted fluorescent microscope Axiovert 135 equipped with a Plan Neo-Fluar 20x/0.75 objective (Carl Zeiss, Inc., Chicago, IL, USA), a digital ECCD camera LucaR (Andor Technology, Belfast, UK), and a hand-made computer-controllable epi-illuminator with a set of light-emitting diodes, particularly allowing for the excitation of Fluo-8 at 480±10 nm. Fluo-8 emission was collected at 535±25 nm. Serial fluorescent images were usually captured every second and analyzed using Imaging Workbench 6 software (INDEC BioSystems, Los Altos, CA, USA). Deviations of cytosolic $Ca^{2+}$ from the resting level in individual Fluo-8 loaded cells was quantified by the ratio $\Delta F/F_0$, where $\Delta F = F - F_0$, $F$ is the instant intensity of cell fluorescence, and $F_0$ is the intensity of cell fluorescence obtained in the very beginning of a recording and averaged over a 20-s interval. All chemicals were applied by the complete replacement of the bath solution in the photometric chamber for nearly 2 s using a perfusion system driven by gravity.

## ATP release assay

ATP release from the CV papilla was monitored on-line by using an Ussing-like chamber and the luciferin-luciferase approach. The horizontally placed chamber included two individually perfused cells with coaxial holes that were adjusted to tightly mount a fragment of the lingual epithelium with the CV papilla (Supplementary Fig. 1S). The mucosal side of the CV preparation was oriented to the upper (mucosal) cell that was filled with the mucosal solution (mM): 50 NaCl, 20 KCl, 2 $CaCl_2$, 0.5 $MgCl_2$, 10 HEPES, and pH 7.6. The tastants were dissolved in the mucosal solution and applied at the rate of ~1 ml/min by using a gravity-driven perfusion system. The bottom (serosal) cell was filled with the serosal solution (135 NaCl, 5 KCl, 2 $CaCl_2$, 1 $MgCl_2$, 10 glucose, 10 HEPES, and pH 7.6) containing 10 µM luciferin (Promega, Madison, WI , USA ) and 0.1 µg/ml luciferase (Promega). Notably, ATP released from a CV papilla upon taste stimulation was hydrolyzed by luciferase, yielding AMP that inhibited the luciferin-luciferase reaction (Fig. 2SB). Therefore, the luciferin-luciferase mixture in the serosal cell was renewed prior to each subsequent taste stimulation of a CV papilla.

The whole chamber with a tightly mounted CV papilla was attached to a photometer (model 814, Photon Technology International (PTI), Lawrenceville, NJ, USA), so that ATP-dependent bioluminescence of luciferin could be captured by a photomultiplier tube (PMT) (R1527P, Hamamatsuu, Japan). PMT operated in the photon counting mode at a count rate being proportional to an instant concentration of ATP in the serosal cell. The photometer data were collected and analyzed using Felix32 software (PTI).

In the very beginning of each recording, a CV preparation was shortly stimulated by 1 µM ATP to check leakage from the mucosal cell into the serosal cell. The absence of detectable PMT signals was considered a criterion indicative of sufficient integrity of a given epithelium preparation because ATP in the serosal cell was reliably detected at as low as 0.1 nM level (Fig. 2SA). Experiments were carried out at RT.

## Chemicals

All used salts, buffers, and bitter compounds were purchased at Sigma-Aldrich; 2-aminoethoxy-diphenylborate (2-APB), GSK 1702934A, and Pyr 10 were from Tocris (Bristol, UK); 1-oleoyl-2-acetyl-*sn*-glycerol (OAG) and 1,2-dioctanoyl-*sn*-glycerol (DOG) were from Abcam (Waltham, MA, USA). Given that the physiological activity of the DAG analogs decreased quickly in physiological saline, these compounds were added to the bath solution immediately before use.

## RT-PCR

Total RNA was routinely isolated from several dozens of individual taste buds, which were extracted from the CV or foliate papilla by using a suction pipette, using RNeasy Mini Kit (Düsseldorf, Germany) according to the manufacturer's protocol. Reverse transcription was performed with Super-Script IV reverse transcriptase (Invitrogen) and random

hexamer primers. PCR amplification of TRPC transcripts was performed using Phusion Hot Start II High-Fidelity DNA Polymerase (Thermo Fisher Scientific, Waltham, MA, USA) and gene-specific primers (Supplementary Table S1). The primers were intron-spanning and designed to recognize sequences of all known splice variants of TRPC transcripts.

### Immunohistochemistry

Isolated mouse tongues were fixed with 4% paraformaldehyde in 0.14 M phosphate-buffered saline (PBS) at 4°C for 2 h. The fixed lingual tissue containing a CV papilla was rinsed with PBS for 20 min and incubated in the embedding medium Tissue-Tek® O.C.T. Compound (Sakura, Torrance, CA, USA) at 4°C for 16 h. Thereafter, 9–11 µm cryostat sections were cut and mounted onto Superfrost Plus slides (Thermo Fisher Scientific, Waltham, MA, USA).

For antigen retrieval, lingual sections were first rinsed by distilled $H_2O$ several times for 10 min at RT and then incubated in PBS containing 0.02% Tween for 2 min. Next, they were incubation in the BlockPRO™ Protein-Free Blocking Buffer (Visual Protein, Taipei, Taiwan) at RT for 1 h. After blocking, slides were rinsed with PBS for 2 min, dried and subjected to the overnight treatment either with the cocktail of rabbit anti-TRPC3 (1:200) (Sigma-Aldrich, St. Louis, MO, USA) and sheep anti-ENTPD2 (1:100) (AF5797, R&D Systems, Minneapolis, MN, USA) or with the mixture of anti-TRPC3 (1:200) and sheep anti-SNAP25 (1:100) (AF5946, R&D Systems) at 4°C. The unbound primary antibodies were removed by rinsing the slices with PBS+0.02% Tween-20 for 15 min. Thereafter, the lingual preparations were exposed to the mixture of anti-sheep IG (1:500) (A-11015, Invitrogen, Waltham, MA, USA) and anti-rabbit IgG (1:500) (711-606-152, Jackson ImmunoResearch, Cambridgeshire, UK) for 2 h at RT, and then unbound antibodies were removed with PBS+0.02% Tween-20 within 25 min. Finally, lingual sections were dried and treated with SlowFade™ Diamond Antifade Mountant (Invitrogen), a liquid mountant protecting fluorescent molecules from fading. All procedures with fluorescent species were performed under weak red light. Immunofluorescent imaging was carried out using a Leica TCS SP5 confocal microscope.

## Results

### Responses of taste cells to DAG analogs

Among diverse ion channels operating in a lipid-dependent manner, solely TRPC2, TRPC3, TRPC6, and TRPC7 have been reported as directly gated by DAG [7, 64]. To elucidate whether some DAG-gated channels might operate in taste cells, we studied their electrophysiological responses to DAG analogs. Cells were isolated from mouse CV and foliate papillae and assayed with the perforated patch approach. Taste cells were identified individually based on exhibited sets of voltage-gated (VG) currents [58, 60, 66]. Taste cells were dialyzed with 140 mM CsCl: this allowed for both to be more unambiguous, compared to KCl dialysis, identification of taste cells [58], and monitoring of activity of TRPC channels, which are well permeable to $Cs^+$ ions [50]. Cells were held at −70 mV and polarized by 100-ms voltage pulses between −100 and 50 mV with the 10-mV decrement. Under these recording conditions, type II cells exhibited inward VG $Na^+$ currents and slowly activating outward currents accompanied by slowly inactivating tail currents (Fig. 1A, left panel), both being mediated by non-selective CALHM1/CALHM3 channels [41, 60]. In type III cells, marked VG $Na^+$ currents were observed, whereas VG outward currents, normally carried by $K^+$ ions through VG $K^+$ channels, were inhibited by internal $Cs^+$ (Fig. 1B, left panel). The absence of evident VG currents was characteristic of type I cells (Fig. 1C, left panel).

Current responses of identified taste cells to DAG analogs were examined at −50 mV, the holding potential allowing both appropriate stability and sufficient sensitivity of recordings. In most cases, cells were treated with 1-oleoyl-2-acetyl-*sn*-glycerol (OAG), although 1,2-dioctanoyl-*sn*-glycerol (DOG) was also used, and both were applied at 100 µM. Given that 50-mM stocks of these compounds were prepared with DMSO, all assayed cells were also treated with 0.2% DMSO in the bath solution as a control. Overall, 27 cells of the type II from CV papillae were found to allow for the conclusive assay. Among them, 15 cells (56%) generated inward current transients of 10–30 pA on OAG (11 cells) (Fig. 1A, right panel) or DOG (4 cells), while none of them detectably responded to 0.2% DMSO (Fig. 3SA). In type III cells ($n$=16), neither OAG nor 0.2% DMSO elicited reproducible current responses that could be clearly distinguished from spontaneous current deviations (Fig. 1B, right panel). Of type I cells assayed in this series (14 cells), most did not respond to the stimulation (Fig. 1C, right panel), although OAG elicited small current transients of 5–7 pA in 4 cells (28 %). Given however that in control, all these cells similarly responded to 0.2% DMSO (Fig. 3SB), their current responses were hardly mediated by DAG-gated channels. Perhaps, DMSO nonspecifically affected a cell-pipette interface and therefore gigaseal, thereby slightly increasing a leakage current. Although taste cells from the foliate papillae were not assayed on the regular basis, they also were found to respond to 100 µM OAG in subtype-specific manner (Fig. 4S), as was the case with CV taste cells (Fig. 1). To all appearance, the functional expression of DAG-sensitive channels is restricted exclusively to taste cells of the type II, at least in the CV and foliate papillae.

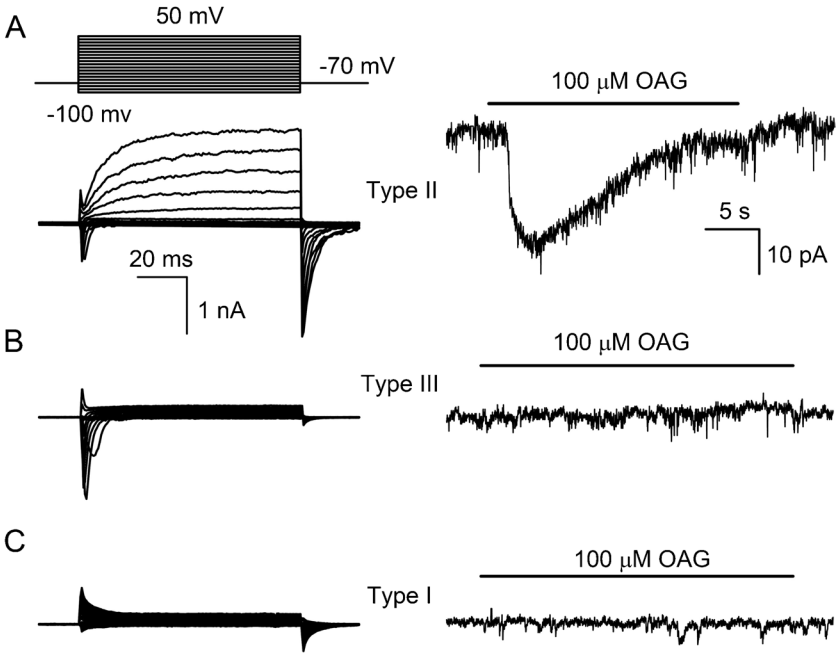


**Fig. 1** Effects of OAG on resting currents in identified taste cells. Left panels, representative families of current responses to electrical stimulation of taste cells of the type II (**A**), type III (**B**), and type I (**C**). Cells were held at −70 mV and polarized from −100 to 50 mV by 100-ms voltage pulses applied with the 10-mV decrement. Right panels, representative effects of 100 μM OAG on resting currents recorded in the same taste cells at −50 mV. Here and below, the compound applications are indicated by the horizontal lines above the experimental traces

## RT-PCR and immunohistochemistry

In line with the physiological findings (Fig. 1), we wondered which TRPC members, including those gated by DAG, could be expressed in taste cells. To minimize a possible contribution of non-taste lingual tissues to total RNA, it was isolated from a preparation of taste buds, which were individually sucked from mouse CV ($n$=4) or foliate ($n$=2) papillae. In all these samples, transcripts of *TRPC1*, *TRPC3, TRPC4*, and *TRPC5* were detected, while transcripts of *TRPC2*, *TRPC6*, and *TRPC7* were not (Fig. 2A). This suggested that among DAG-gated TRPC2/3/6/7 channels, only TRPC3 is expressed in taste cells from the mouse CV and foliate papillae.

To confirm this inference, immunohistochemistry experiments were performed using tongue sections containing the CV papilla. Given that functional evidence locates the expression of DAG-gated channels in type II cells (Fig. 1), this cellular subgroup rather than type I and type III cells was expected to exhibit TRPC3-like immunoreactivity. Therefore, co-expression of TRPC3 and NTPDase2 or SNAP 25, the conventional surface markers for taste cells of the type I and type III, respectively [29], was analyzed. The CV sections were treated with primary TRPC3 antibody in combination with antibody against either NTPDase2 ($n$=17) or SNAP 25 ($n$=9). Thereafter, the sections were exposed to an appropriate mixture of secondary antibodies conjugated with Alexa Fluor 488 (NTPDase2/SNAP 25) and Alexa Fluor 647 (TRPC3).

In mammalian taste buds, a cell population is roughly composed of type I cells by half and type II cells by one third [61, 72]. Consistently with this distribution, nearly half taste bud cells seen on CV sections exhibited NTPDase2 immunoreactivity (IR), while cells with TRPC3-IR were much less abundant (Fig. 2B). In merged images of NTPDase2-IR and TRPC3-IR cells, apparently, none of them exhibited clearly overlapped green and red immunofluorescence (Fig. 2B). Together, these findings and that the activity of DAG-gated channels was not detected in type I cells (Fig. 1C) indicated that type I cells hardly express the TRP3 protein. Taste bud cells showing SNAP-25-like IR were more numerous (Fig. 2C) than expected for type III cells, as their fraction does not exceed 20% [61, 72]. Perhaps, SNAP-25 expression is not restricted merely to type III cells. Indeed, although type I cells are considered to perform largely supportive and/or glia-like functions [61, 65], membrane-bound dense granules have been identified in their apical pole [37, 44]. Hence, it cannot be excluded that a fraction of type I cells fulfills a secretory function. If so, the presence of SNAP-25 in certain type I cells is physiologically relevant, and it accounts for the previously reported detection of SNAP-25 transcripts in a subpopulation of individual cells of the type I [10]. In any case, quantitatively, cells exhibiting TRPC3 were much more abundant compared to cells that appeared as IR to both TRPC3 and SNAP (Fig. 2C). This indicates that SNAP-25-positive cells are generally TRPC3-negative. Thus, the immunohistochemical analysis data (Fig. 2) were consistent with the electrophysiological findings (Fig. 1), and both evidenced that DAG-gated TRPC3 channels are primarily expressed in type II cells.

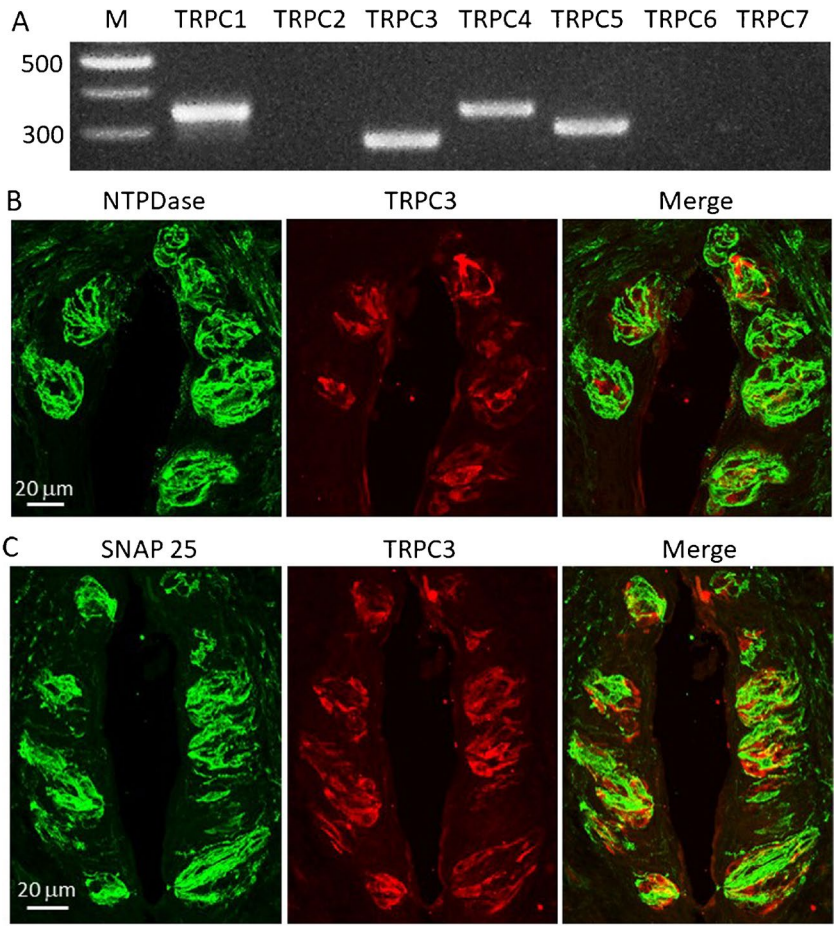


**Fig. 2** Expression of TRPC channels in mouse CV papillae. **A** Representative RT-PCR detection ($n$=4) of TRPC transcripts in RNA preparation extracted from taste buds isolated from a CV papilla. The bands seen in the electrophoregram confirm the expression of *TRPC1* (352 bp), *TRPC 3* (268 bp), *TRPC4* (343 bp), and *TRPC5* (309 bp); amplicons for *TRPC2* (326 bp), *TRPC6* (260 bp), and *TRPC7* (417 bp) were not detected. The molecular weight markers (M) were Gene Ruler 100 bp Ladder (Fermentas). The 1.2% agarose gel was stained with ethidium bromide. **B** Representative immunostaining of the same tongue section containing CV taste buds ($n$=9) with a combination of antibodies. The primary staining was performed with rabbit TRPC3 antibody and sheep NTPDase2 antibody. The secondary antibody was donkey anti-rabbit and anti-sheep IgG conjugated with Alexa Fluor 488 (left panel) and Alexa Fluor 647 (middle panel), respectively. **C** Representative ($n$=5) TRPC3- and SNAP 25-like immunoreactivity of taste bud cells in the same tongue section. The section was stained as in **B** except for that the NTPDase2 antibody was substituted for primary rabbit antibody against SNAP 25

It is noteworthy that findings described below implicated TRPC3 in taste transduction and suggested this channel to be located apically. In almost all taste bud sections, the apical tips were not clearly apparent due to small (~5 µm) size of the taste pore (Fig. 2B, C)**.** Nevertheless, among 26 CV sections subjected to immunostaining, we found two taste buds with apparently intact apical protrusions that exhibited TRPC3-IR (Fig. 5S). Although this very uncommon TRPC3-IR pattern cannot be considered as sufficient evidence, it points out that the apical membrane can be a primary cite for TRPC3. Additional experiments are required to validate this suggestion.

## Responses of taste cells to bitter stimuli and OAG

In designated experiments, we clarified whether DAG-gated channels, presumably TRPC3, are involved in taste transduction in type II cells. In this series, cells were isolated solely from CV papillae, and taking into account their taste specialization, individual cells were stimulated by the bitter mix of cycloheximide (20 µM), 6-n-propylthiouracil (100 µM), phenylthiocarbamide (50 µM), and sucrose octaacetate (500 µM). Overall, 52 sufficiently robust cells of the type II were assayed, 23 of which (44%) responded to both the bitter stimulus and 100 µM OAG by generating inward current transients at −50 mV (Fig. 3A). Notably, nonselective large-conductance CALHM channels, which are activated strongly by depolarization, rendered the plasmalemma of

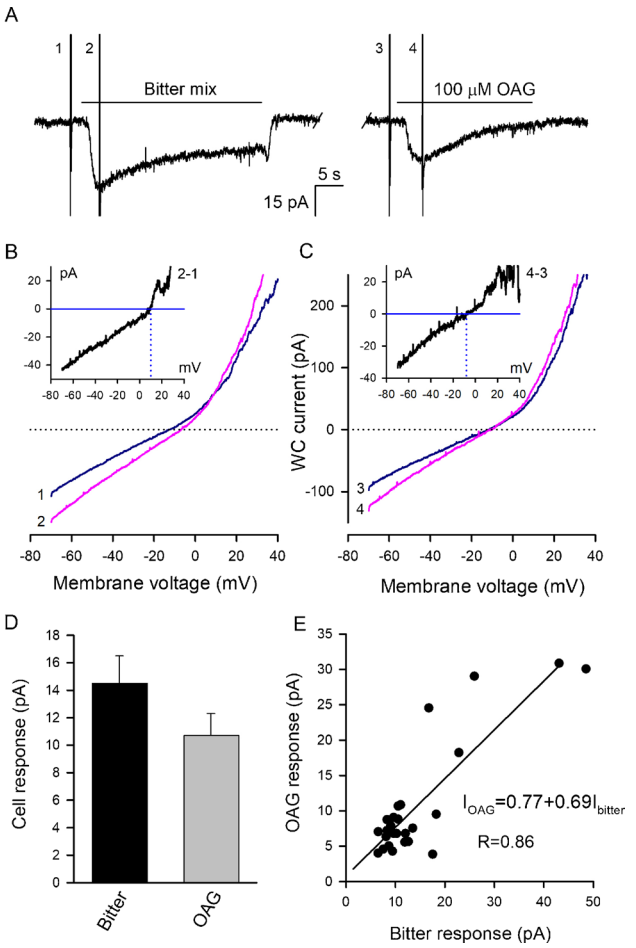


**Fig. 3** Current responses of type II cells. **A** Representative responses of a cell held at −50 mV and sequentially stimulated by the bitter mix and 100 μM OAG in the presence of 10 μM TTX. Current transients 1–4 were produced by the voltage ramp applied to generate I–V curves. **B, C** I–V curves generated at the moments 1–4 in **A**. Insets, I–V curves for the bitter-sensitive current and OAG-gated current, which were calculated as the difference between curves 2 and 1 and curves 4 and 3, respectively. **D** Averaged bitter and OAG responses, presented as a mean±SD ($n$=23). **E** OAG response versus bitter response plotted for 23 individual cells. The straight line represents the linear regression of the experimental data

type II cells highly permeable to both cations and anions at positive voltages (Fig. 1A, left panel). For this reason, the accurate evaluation of selectivity of the small bitter- or DAG-sensitive conductance (Fig. 3A) by manipulating ions in the bath was unfeasible. Instead, we characterized current responses to the substances by generated I-V curves using a voltage ramp (1 mV/ms) to polarize cells from −70 to 40 mV just prior to chemical stimulation and when a cell response peaked (Fig. 3A, current transients 1–4). Given that the voltage ramp produced sufficiently high VG $Na^+$ currents, cell responsivity was studied in the presence of 10 μM TTX to suppressed VG $Na^+$ channels in type II cells. The representative I–V curves generated in this manner are shown in Fig. 3 B and C. For the bitter- and DAG-sensitive currents, the I-V curve was calculated as a difference between curves 2 and 1 (Fig. 3B, inset) and curves 4 and 3 (Fig. 3C, inset), respectively.

It turned out that bitter-sensitive currents reversed at 10–20 mV (Fig. 3B, inset) ($n$=23) under the (140 mM $CsCl)_{in}$/(140 mM $NaCl)_{out}$ gradient, while reversal potentials of OAG-elicited currents were more negative and ranged within −10–0 mV ($n$=23) (Fig. 3C, inset). Usually, bitter responses exceeded OAG responses by nearly 35% on average (Fig. 3D). As the bitterness- and OAG-evoked currents differed in magnitudes and reversal potentials, each could be mediated by a specific set of ion channels. On the other hand, bitter- and OAG responses correlated strongly, as indicated by OAG responses plotted versus bitter responses: the linear regression of the resultant set of points gave the correlation coefficient $R$=0.89 (Fig. 3E).

Altogether, the abovementioned findings pointed out the possibility that the DAG-gated current could represent a fraction of the generator current initiated by taste stimulation. Given that TRPC channels are well permeable to $Ca^{2+}$ [50], DAG-gated channels could provide sufficiently high $Ca^{2+}$ influx in type II cells. If so, both $Ca^{2+}$ release mediated by the type 3 $IP_3$ receptor and $Ca^{2+}$ influx through TRPC3 could contribute to a tastant-triggered $Ca^{2+}$ signal that governed the transduction channel TRPM5.

To verify the abovementioned possibility, we analyzed the influence of bath $Ca^{2+}$ and therefore $Ca^{2+}$ entry, on $Ca^{2+}$ mobilization associated with taste transduction. Using the $Ca^{2+}$ dye Fluo-8 and $Ca^{2+}$ imaging, we explored $Ca^{2+}$ signaling both in individual taste cells and at the level of isolated taste buds. Although in the last case, the total $Ca^{2+}$ signal could not be attributed exclusively to type II cells, the advantage of this cell preparation was that all taste buds ($n$=22) responded to the bitter stimulation (Fig. 4A). Being quite pronounced under pseudo-physiological conditions, bitter responses of the taste buds reversibly decreased at 2 μM $Ca^{2+}$ in the bath (Fig. 4A, C). This observation implied that $Ca^{2+}$ entry into taste cells might be critically important for generation of $Ca^{2+}$ responses to bitter stimulation. Interestingly, 100 μM OAG also triggered $Ca^{2+}$ signals in individual taste buds, which developed slower but was rather close to the taste responses by magnitude (Fig. 4A, C).

Overall, 98 individual taste cells were assayed with $Ca^{2+}$ imaging. Among them, 17 cells (18%) responded to the bitter mix, while 70 mM KCl did not elicit $Ca^{2+}$ transients (Fig. 4B), the observation that suggested them to be type II. Similar to the taste buds (Fig. 4A), individual taste cells generated well-resolved $Ca^{2+}$ responses to the bitter mix at 2 mM $Ca^{2+}$ in the bath but were poorly responsive at low extracellular $Ca^{2+}$ (Fig. 4B, D). The bitter-sensitive cells also responded to 100 μM OAG by generating $Ca^{2+}$ transients comparable with bitter responses (Fig. 4B, C). Both

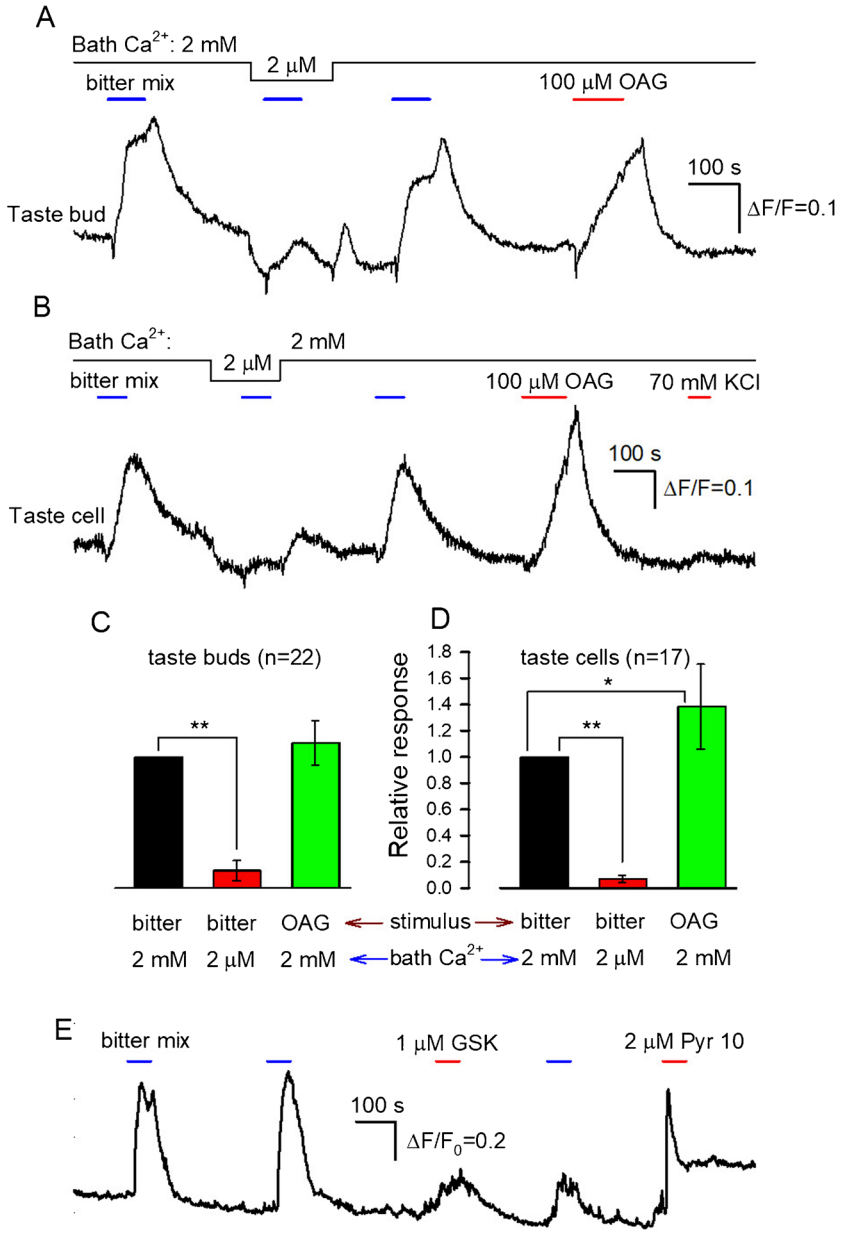


**Fig. 4** Calcium responses to the bitter mix and OAG. **A** Integral fluorescence of an individual taste bud loaded with Fluo-8. The fluorescence was quantified by the ratio $\Delta F/F_0$, where $\Delta F = F - F_0$, $F$ is the instant intensity of bud fluorescence, and $F_0$ is the intensity of bud fluorescence obtained in the very beginning of a recording and averaged over a 20-s interval. The bath $Ca^{2+}$ varied with time as shown by the continuous line above the recording. The bitter mix (20 µM cycloheximide, 100 µM 6-n-propylthiouracil, 50 µM phenylthiocarbamide, and 500 µM sucrose octaacetate) and 100 µM OAG were applied as indicated. **B** Monitoring of intracellular $Ca^{2+}$ in an individual Fluo-8-loaded taste cell stimulated by the bitter mix and 100 µM OAG. In the ratio $\Delta F/F_0$, $\Delta F = F - F_0$, $F$ is the instant intensity of cell fluorescence, and $F_0$ is the intensity of averaged cell fluorescence in the beginning of a recording. Summary of $Ca^{2+}$ responses of **C** taste buds ($n$=22) and **D** taste cells ($n$=17) to the bitter mix and 100 µM OAG at extracellular $Ca^{2+}$ as indicated. The particular response was calculated as the difference between fluorescence intensities measured immediately before compound application and when it peaked. To compare different recordings, the first bitter response of a particular taste bud or cell was taken as a unit. The data are presented as a mean±SD. The single and doubled asterisks indicate the statistically significant difference at $p<0.05$ and $p<0.01$, respectively. **E** Monitoring of intracellular $Ca^{2+}$ in a type II cell treated with the bitter mix and TRPC3 ligands

the pronounced sensitivity of bitter responses to extracellular $Ca^{2+}$ and the ability of OAG to stimulate $Ca^{2+}$ transients in bitter responsive cells supported the idea that taste transduction could involve not only $IP_3$-driven $Ca^{2+}$ release but also $Ca^{2+}$ influx through DAG-gated channels, presumably, TRPC3 (Fig. 2).

To verify TRPC3 activity in taste cells, we assayed their sensitivity to the selective TRPC3/6 activator GSK 1702934A ($EC_{50}$~100 nM) and selective TRPC3 inhibitor Pyr 10 ($IC_{50}$~0.7 μM) [62, 71]. Although the TRPC3 agonist (1 μM) expectedly elevated cytosolic $Ca^{2+}$ (5 cells) (Fig. 4D), the GSK-evoked $Ca^{2+}$ transients were subtle compared to bitter- and OAG responses (Fig. 4B, D). Moreover, GSK irreversibly suppressed responsiveness of taste cells to the bitter mix (Fig. 4D). Surprisingly, 2 μM Pyr 10 initiated $Ca^{2+}$ bursts followed by a sustained rise in cytosolic $Ca^{2+}$ (8 cells) (Fig. 4D). It thus appeared that both GSK and Pyr 10 caused unspecific effects, and therefore, these TRPC3 ligands could not be used as a reliable tool for validating TRPC3 activity in type II cells.

It is noteworthy that the bitter mix used in our experiments elicited relatively slow $Ca^{2+}$ responses in type II cells, which developed within 30–100 s at room temperature (Fig. 5A). The similar slow kinetics of bitter responses has been observed in previous studies of isolated taste cells [11, 16, 42]. On the other hand, taste cells in lingual slices responded to taste stimuli for 10–20 s [12, 13]. However, these recordings were performed at 30 °C and with 8 mM $Ca^{2+}$ in the bath, the factors that could accelerate $Ca^{2+}$ responses. Importantly, in our experiments, type I cells generated much more rapid $Ca^{2+}$ responses to purinergic agonists by involving P2Y receptors coupled to the phosphoinositide cascade [6]. In this case, largely $Ca^{2+}$ release formed cellular responses, which peaked for few seconds (Fig. 5B). Comparably fast $Ca^{2+}$ signals also were produced by $Ca^{2+}$ influx through VG $Ca^{2+}$ channels in type III cells, stimulated by 100-ms depolarization (Fig. 5C). The reason for such a dramatic kinetics difference between taste responses of type II cells (Fig. 5A) and the mentioned $Ca^{2+}$ signals in type I and type III cells (Fig. 5B, C) remains unclear. It could simply reflect a technical issue: the non-confocal optics we used could not resolve a taste-related $Ca^{2+}$ response, should it be generated very locally in the close vicinity of the apical membrane. The fast kinetics of current responses to the bitter mix, which usually peaked for few seconds (Fig. 3A), is rather consistent with the idea that taste related $Ca^{2+}$ signals were generated quickly and locally (see also Fig. 2A in [13]). In this case, the resultant global $Ca^{2+}$ signal should have been diminished and slowed compared to the initially rapid and local $Ca^{2+}$ transient.

Although the suppressive effect of low bath $Ca^{2+}$ on the sensitivity of type II cells to the bitter mix (Fig. 4A–C) was well reproducible in our experiments, it is not consistent with some previous reports. Particularly, taste cells, which were assayed ***in situ*** in lingual slices, responded to cycloheximide (10 μM) with $Ca^{2+}$ transients, which were also preserved in nominally $Ca^{2+}$ free bath solution with no added $Ca^{2+}$ and EGTA [13]. Notably, these recordings were performed with 8 mM $Ca^{2+}$ in the bath, and application of nominally $Ca^{2+}$ free bath solution could remove extracellular $Ca^{2+}$ accumulated in a slice preparation insufficiently quickly. In individual type II cells from CV papilla, denatonium (2.5 mM) induced comparable $Ca^{2+}$ transients in both normal and $Ca^{2+}$-free bath solutions, suggesting $Ca^{2+}$ release to be the predominant contributor [52, 55]. We explored responsiveness of taste cells to denatonium as well.

Previously, two subpopulations of bitter responsive cells have been described [25]. While one expectedly included type II cells, another subgroup responded to KCl-induced depolarization with marked $Ca^{2+}$ transients, thus being defined as type III cells only expressing VG $Ca^{2+}$ channels. In our experiments, we identified taste bud cells ($n$=19) that responded to millimolar denatonium by generating relatively high, fast, and oscillatory $Ca^{2+}$ transients (Fig. 5D). Yet, these cells generated negligible $Ca^{2+}$ signals on stimulation with both 70 mM KCl and the bitter mix (Fig. 5D). Given these features, we inferred that these cells represented a fraction of type II cells specifically responsive to denatonium. Although extracellular $Ca^{2+}$ subtly affected amplitudes of denatonium responses (Fig. 5D), the response lag was $Ca^{2+}$ dependent and nearly twice increased at bath $Ca^{2+}$ reduced from 2 mM to 260 nM (Fig. 5E). By relatively high

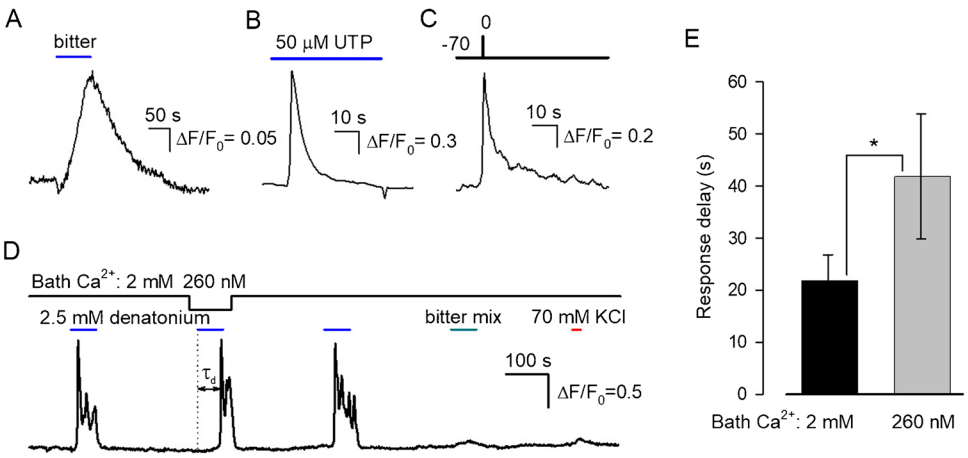


**Fig. 5** Representative $Ca^{2+}$ transients elicited by **A** the bitter mix, **B** 50 mM UTP, and **C** depolarization from −70 to 0 mV in taste cells of the type II, type I, and type III, respectively. **D** Denatonium responses of a taste cell that responded neither to the bitter mix nor to 70 mM KCl. **E** Lag of denatonium responses was inversely dependent on bath $Ca^{2+}$. The characteristic time of the response delay ($\tau_d$) (second response in **B**) was calculated as a time interval necessary for a $Ca^{2+}$ transient to reach the half-magnitude

amplitude (in terms of $\Delta F/F_0$), rapid kinetics, and weak sensitivity to bath $Ca^{2+}$, denatonium responses (Fig. 5D) markedly differed from responses to the bitter mix (Fig. 4B, D). It is therefore likely that the bitter mix and denatonium involved different pathways to trigger $Ca^{2+}$ signaling in type II cells.

## ATP release from CV papilla

The assay of isolated taste buds and cells (Figs. 1, 3, 4, and 5) was disadvantageous in that the used tastants, DAG analogs, channel modulators, and low bath $Ca^{2+}$ affected the whole cell surface rather than specifically the receptive apical membrane. Therefore, the possibility of unspecific, not related to taste, effects could not be excluded.

To address this issue, we elaborated the methodology that allowed for the apical stimulation of taste cells and on-line monitoring of stimulus-induced ATP release, the ultimate phase of taste transduction in type II cells. This approach involved an isolated epithelium fragment containing a CV papilla, which was embedded into a horizontally placed Ussing-like chamber consisting of two separately perfused cells (Supplementary Fig. 1S). The mucosal side of a mounted CV preparation was oriented to the upper (mucosal) cell that was filled with a mucosal solution (see the "Materials and methods" section). The tastants were dissolved in the mucosal solution and applied at the rate of ~1 ml/min by using a gravity-driven perfusion system. The bottom (serosal) cell was filled with a serosal solution that contained a luciferin-luciferase mixture. This allowed for the reliable detection of released ATP at sufficiently low level of about 0.1 nM (Fig. 2SA). Given that the hydrolysis of ATP by luciferase produced AMP, which inhibited the luciferin-luciferase reaction (Fig. 2SB), the luciferin-luciferase mixture was renewed prior to each subsequent taste stimulation of a CV preparation. Luciferin bioluminescence was captured by a photomultiplier tube (PMT) operating in the photon counting mode with a count rate being proportional to the instant concentration of ATP in the serosal cell. In the very beginning of each recording, a CV preparation was shortly stimulated by mucosal ATP (1 μM) to check its integrity, that is the diffusional exchange between the mucosal cell and the serosal cell (Fig. 2SC). The absence of a detectable PMT signal was considered as indicative of the sufficient integrity of the assayed CV preparation, given the high sensitivity of the luciferin-luciferase assay (Fig. 2SA, C).

Using this approach, we succeeded in the detection of transient ATP release from isolated CV papillae ($n$=19) briefly stimulated with bitter substances, while sweeteners, such as saccharine, acesulfame K, aspartame, and neotame, were ineffective. Notably, denatonium and quinine were predominantly used in the below experiments because these compounds could be easily rinsed out of the CV papilla, thus providing the possibility to repeatedly discharge ATP from a CV preparation for up to 1 hr. First, we questioned whether ATP release was dependent on mucosal $Ca^{2+}$. Although the complete removal of $Ca^{2+}$ in the mucosal solution with EGTA significantly diminished bitter-stimulated ATP release, the EGTA effects were poorly reversible and therefore inconclusive (Fig. 2SD). For this reason, some experiments were carried out with a nominally $Ca^{2+}$-free mucosal solution containing no added $CaCl_2$. Presumably, this "$Ca^{2+}$-free" saline contained a trace quantity (<1 μM) of $Ca^{2+}$ ions due to calcium contaminations present in sodium and potassium salts. In this series, we assayed 6 robust CV preparations, and in a typical recording, the 60-s application of 50 mM denatonium ($n$=3) or 20 mM quinine ($n$=3) in the presence of 2 mM $Ca^{2+}$ elicited a significant increase in luciferin bioluminescence (Fig. 6A, 1$^{st}$ response). This signal was transient for several reasons: (i) Being released shortly and locally, ATP was subjected to dilution in the serosal cell; (ii) effective concentration of ATP continuously decreased due to its hydrolysis by luciferase; and (iii) resultant AMP inhibited the luciferin-luciferase reaction (Fig. 2SB).

When a bitter stimulus was applied in the "$Ca^{2+}$ free" mucosal solution, the corresponding ATP response was reduced by 68–76% compared to control (Fig. 6 A, B, 2$^{nd}$ response). Consequent perfusion of a CV preparation with the normal mucosal solution restored its responsivity (Fig. 6A, B, 4$^{th}$ response), indicating that mucosal $Ca^{2+}$ modulated the sensitivity of the CV papilla to the bitter stimulation. Hypothetically, extracellular $Ca^{2+}$ might be a cofactor that promoted activity of bitter receptors, as is the case with GPCRs from the family C [69]. Alternatively, the "$Ca^{2+}$ free" effects could reflect the necessity of $Ca^{2+}$ entry through apical channels for taste transduction. To verify the last possibility, we used 2-APB known to inhibit diverse $Ca^{2+}$ entry channels, including the TRPC members [34]. It turned out that 50 μM 2-APB almost completely but reversibly suppressed bitter-induced ATP release in all five CV preparations tested (Fig. 6C, D). It was also found that at the concentration of 10 μM and higher concentrations, the TRPC3 inhibitor Pyr 10 suppressed tastant-stimulated ATP release completely but irreversibly. At 2 μM, Pyr 10 reduced ATP release reversibly but solely by 51±8% on average ($n$=4) (Fig. 6E, D).

Altogether, the effects of mucosal $Ca^{2+}$, 2-APB and Pyr 10 on ATP release (Fig. 6) supported the idea that bitter transduction in type II cells involves $Ca^{2+}$ entry through DAG-gated TRPC3 channels. Another supporting evidence was that 500 μM DOG applied from the mucosal side also stimulated ATP secretion, although less effectively than 20 mM quinine ($n$=4) (Fig. 7A, B). In the plasma membrane, agonist-stimulated PLC generates sn-1,2 DAG, and this DAG stereoisomer is largely metabolized by DAG

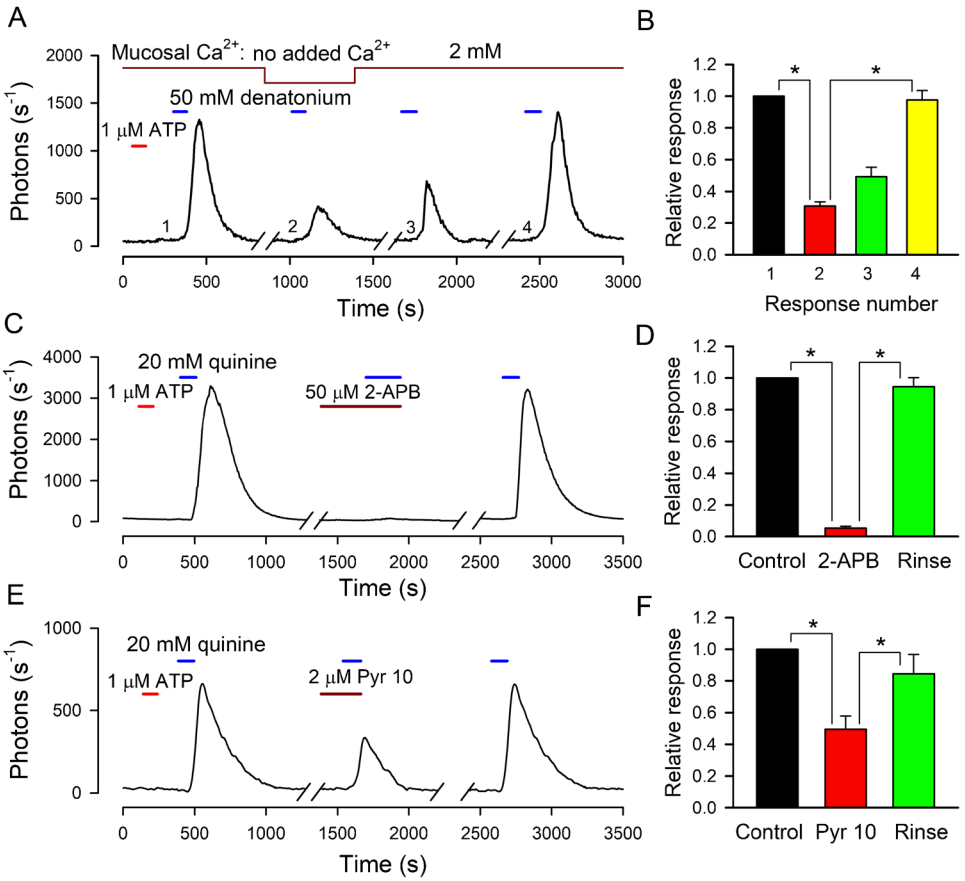


**Fig. 6** On-line monitoring of ATP release ***in situ***. **A** Luciferin-luciferase response associated with ATP release from a CV papilla stimulated by 50 mM denatonium was markedly impaired at low $Ca^{2+}$ in the mucosal solution. **B** Summary of sequential luciferin-luciferase responses to 50 mM denatonium in control (response 1), at low $Ca^{2+}$ (response 2), and after recovery of mucosal $Ca^{2+}$ (responses 2 and 3). The data are presented as a mean±SD ($n$=6). **C** 2-APB (50 μM) completely and reversibly suppressed ATP release stimulated by 20 mM quinine. **D** Summary of effects of mucosal 2-APB on luciferin-luciferase responses to 20 mM quinine ($n$=3). **E, D** TRPC3 antagonist Pyr 10 reversibly suppressed ATP secretion induced by 20 mM quinine ($n$=4). In **B, D, and F**, the asterisks indicate the statistically significant difference at **B, F** $p$<0.005 or **D** $p$<0.001

kinases and DAG lipases [20]. We therefore expected that the inhibition of either of these DAG-metabolizing enzymes should have enhanced stimulus-evoked DAG transients and therefore $Ca^{2+}$ entry through DAG-gated channels, thereby enlarging induced ATP release. It turned out that the addition of the DAG lipase inhibitor HCR80267 (2 μM) to the mucosal solution led to a nearly threefold increase in the magnitude of ATP release (Fig. 7C, D). In contrast, the DAG kinase inhibitor R59022 did not enhance stimulated ATP release but instead, it promoted rundown of ATP secretion at 2 μM ($n$=4) (Fig. 7E, F). At 50 μM, R59022 irreversibly suppressed responsivity of CV preparations ($n$=2) (Fig. 7G, H), suggesting that the effects of this DAG kinase inhibitor were mostly nonspecific. Altogether, the abovementioned findings (Figs. 6 and 7) indicated that taste transduction involves DAG signaling terminated by DAG lipase to regulate $Ca^{2+}$ entry at least.

## Discussion

Intracellular $Ca^{2+}$ is a key regulator of transduction machinery in diverse sensory cells, including retinal photoreceptors, sensory neurons in the main olfactory epithelium and vomeronasal organ, and hair cells in the Corti organ. Crucial for $Ca^{2+}$ signaling initiated by sensory stimuli in receptive compartments is $Ca^{2+}$ entry through specialized transduction channels responsible for generation receptor potential.

In retinal rods and cones, phototransduction involves cation channels directly gated by cGMP [22]. Several key transduction proteins are negatively regulated by cytosolic $Ca^{2+}$, including cGMP-gated channels, guanylyl cyclase producing cGMP, and rhodopsin kinase that determines the lifetime of active rhodopsin. By these $Ca^{2+}$-dependent regulations, $Ca^{2+}$ influx via cGMP-gated channels is central to maintaining both the dark steady-state and light adaptation in rods and cones [73].

Sounds and head movement are detected by hair cells that are sensitive to mechanical deflection of their hair bundles. The mechano-electric transduction (MET) involves MET channels responsive to mechanical distortion of stereocilia, wherein transduction machinery is localized [23, 40]. The adaptation of hair cells to a sustained hair-bundle displacement exhibits fast and slow modes, both involving $Ca^{2+}$ influx through the MET channels [23, 24].

In the main olfactory epithelium, transduction of most odorants involves the cAMP-signaling pathway operating in cilia of olfactory sensory neurons (OSNs). The binding of odorous molecules to specialized GPCRs, which are coupled to adenylate cyclase 3 by $G_s$-proteins $G_{olf}$, produces a burst of cAMP in the olfactory cilia [3]. This second messenger

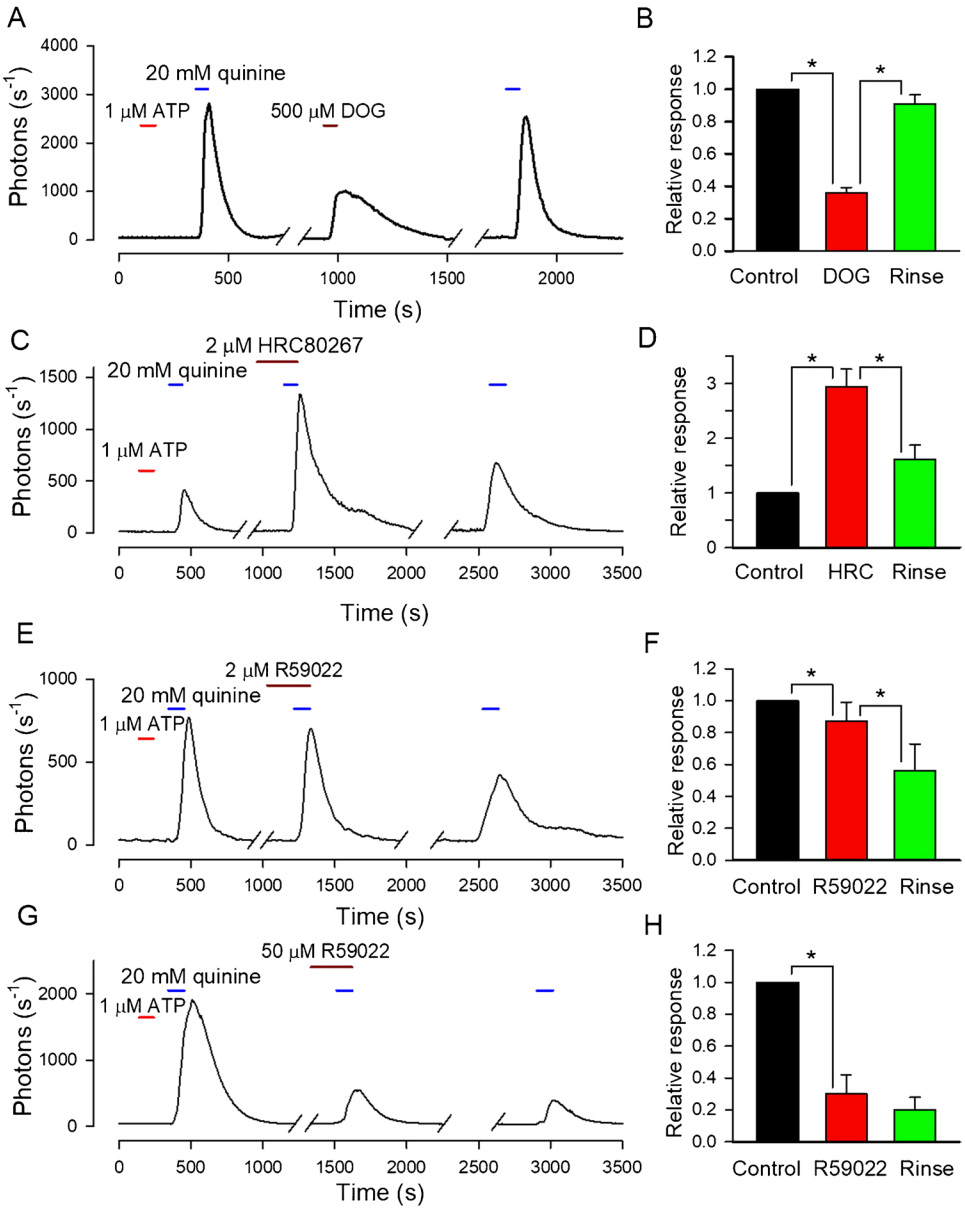


**Fig. 7** Stimulated ATP secretion under different conditions. **A, B** DAG analog DOG (500 µM) was capable of stimulating ATP release but less effectively than 20 mM quinine ($n$=4). **C, D** DAG lipase inhibitor HCR80267 (2 µM) initiated a nearly three-fold increase in ATP release. **E–H** Effects of the DAG kinase inhibitor R59022 at different doses. In **B, D, F, and H**, the data are presented as a mean±SD. The asterisks indicate the statistically significant difference at **B, D** $p$<0.001, **F** $p$<0.03, and **H** $p$<0.01

opens cyclic nucleotide-gated (CNG) channels that mediate influx of $Na^+$ and $Ca^{2+}$ ions to depolarize OSN [32, 47]. Odorant-induced $Ca^{2+}$ entry through the CNG channels elevates cilial $Ca^{2+}$ and stimulates nearby $Ca^{2+}$-gated $Cl^-$ channels, so that $Cl^-$ efflux amplifies the initial OSN depolarization [17]. In addition, $Ca^{2+}$/CaM regulates cAMP turnover and CNG channels, thereby providing the basis for olfactory adaptation [75].

Sensory neurons operating in the vomeronasal organ (VNO) detect pheromones by employing specialized GPCRs. Irrespective of VNO neuron specialization, pheromone transduction involves the stimulus-dependent cleavage of $PIP_2$ by PLC, PLCβ2 or PLCβ4, thus producing soluble $IP_3$ and membrane-bound DAG. While $IP_3$ signaling is basically directed at the regulation of $Ca^{2+}$ release trough $IP_3$Rs [8], DAG signaling is more diverse. It particularly includes the direct regulation of certain membrane processes, e.g. $Ca^{2+}$ entry, as well as pathways involving downstream DAG derivatives, such as arachidonic acid, which are characterized by their own circuits [20]. Based on the PLC-dependent lipid turnover, several mechanisms have been proposed to account for the responsivity of VNO neurons to pheromones [63]. As being expressed and abundant in sensory microvilli of VNO neurons, DAG-gated TRPC2 channels have been implicated in pheromone transduction [35, 43]. Evidence exists that entry of external $Ca^{2+}$ through TRPC2 is central to $Ca^{2+}$ signaling stimulated by pheromones in individual VNO neurons, while $IP_3$-mediated $Ca^{2+}$ release or $Ca^{2+}$ entry via arachidonate-regulated $Ca^{2+}$- channels contribute subtly or negligibly [39].

Thus, diverse sensory cells universally rely on $Ca^{2+}$ entry through transduction channels to control the amplification and adaptation of transduction machinery. By this mode, taste transduction appears to be distinct. Indeed, in line with the current concept of taste transduction, just the TASR/PLCβ2/$IP_3$R3/TRPM5 axis provides chemo-electrical coupling in type II cells [61, 65]. While this pathway necessarily involves stimulus-dependent $IP_3$ generation and $Ca^{2+}$ release through $IP_3$R3, DAG appears to be a byproduct of $PIP_2$ cleavage by PLCβ2. In addition, the transduction channels TRPM5 are not permeable to $Ca^{2+}$, so that a mechanism of taste-related $Ca^{2+}$ entry and its possible role in taste transduction remain obscure.

The recent report [45] and our findings presented here suggest that DAG-signaling, DAG-regulated $Ca^{2+}$ entry leastwise, could represent an important, not yet recognized factor in taste transduction. In particular, we demonstrated the following: (i) DAG-gated channels, presumably TRPC3, are functionally expressed in type II cells (Figs. 1 and 2); (ii) DAG-gated current constitutes a fraction of a generator current elicited by taste stimulation (Fig. 3); (iii) bitter stimuli and DAG analogs trigger $Ca^{2+}$ transients in type II cells, which are greatly diminished at low bath $Ca^{2+}$ (Fig. 4); and (iv) being initiated ***in situ*** by bitter stimuli and DAG analogs, ATP release from taste buds is substantially decreased at low $Ca^{2+}$ in the mucosal solution (Fig. 6).

In all known sensory cells, molecular sensors and transduction pathways are localized in specialized organelles, such as outer segments in rods and cones, olfactory cilia in olfactory sensory neurons, stereocilia in hair cells, and microvilli in VNO neurons. The recent morphological reconstruction of CV taste buds suggests that a Type II cell is commonly crowned with a single sufficiently long (~10 μm) microvillus [70, 72], which presumably has the sensory function and bring taste GPCRs coupled to the downstream phosphoinositide cascade [38]. Microvilli are present on the surface of almost all differentiated cells, being usually of ~1 μm length and 0.1 μm in diameter [31]. Evidence exists that microvilli contains 19 actin microfilaments, which are cross-linked by fimbrin and villin and laterally tethered by multiple myosin/calmodulin cross-bridges to the adjacent membrane [9]. This filamentous net leaves no room for any organelles, including $Ca^{2+}$ store, inside of a microvillus [31]. Although the structural organization of microvilli in type II cells has not been elucidated yet, it is likely that taste-related $Ca^{2+}$ store and $IP_3$-dependent $Ca^{2+}$ release localize outside of the microvillar compartment, as suggested in Fig. 8. If so, $IP_3$ produced by taste stimulation in the microvillus should diffuse for nearly 5 μm on average to reach $IP_3$R3s.

The diffusion of substances in a microvillus is virtually one-dimensional, and the characteristic time of $IP_3$ diffusion τ could be evaluated using the appropriate variant of the Einstein equation $l^2=2D\tau$. In the cell cytosol, diffusion is complicated by the macromolecule crowding, binding, and volume exclusion due to macromolecular complexes, intracellular cytoskeleton, and organelles, so that the reported values of the diffusion coefficient for $IP_3$ vary within 10–300 $\mu m^2/s$ [56]. Even for minimal $D$=10 $\mu m^2/s$, $\tau=l^2/2D \approx 1$ s at $l$=5 μm. As a comparison, the $PIP_2$ depletion by PLC takes several seconds even at saturating stimulation of a cell [21, 26, 28]. Both estimates imply that $IP_3$ diffusion could hardly limit the kinetics of activation of IP3Rs even if they are located outside the microvillus (Fig. 8).

The $PIP_2$ level in a microvillus is largely determined by a balance between the PLC-mediated hydrolysis of $PIP_2$ and its recovery, which occurs primarily through the sequential phosphorylation of phosphatidylinositol [19]. The last process is relatively slow. For instance, in CHO cells stimulated by muscarinic agonists at saturating concentrations, $PIP_2$

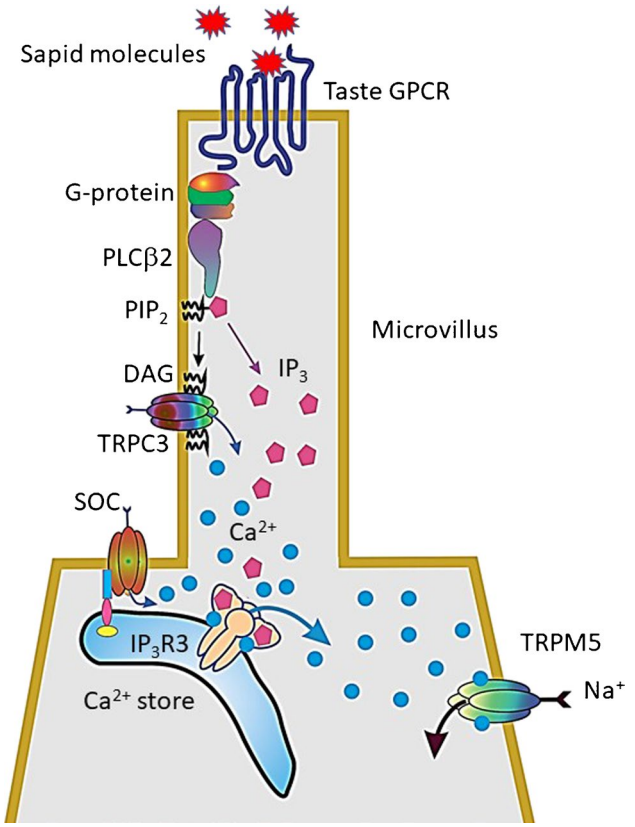


**Fig. 8** Model of $IP_3$/DAG signaling in a taste cell of the type II. Being rendered active by sapid molecules, taste GPCRs initiate $PIP_2$ cleavage by PLCβ2 to produce $IP_3$ burst and more prolonged DAG signal in a cilium. The diffusion removes $IP_3$ from the cilium to trigger $Ca^{2+}$release trough $IP_3$R3s located outside the compartment, thus forming the initial transient phase of a taste related $Ca^{2+}$ signal. DAG remains in the cilium and stimulates TRPC3 channels, which mediate, presumably in concert with store-operated $Ca^{2+}$ channels (SOCC), sustained $Ca^{2+}$ entry, thus prolonging the initial $Ca^{2+}$ transient. This $IP_3$R3/TRPC3/SOCC-mediated $Ca^{2+}$ signal initiates and maintain activity of TRPM5

was depleted within few seconds to 7% of control [28], while $PIP_2$ recovery took nearly 100 s [18, 21, 46]. Similar data have never been reported for taste cells, so that the dynamic features of taste-related $IP_3$-signaling remain uncertain. Nevertheless, based on the abovementioned estimates, the following plausible scenario could be suggested. Being initiated by taste stimulation of a type II cell, a burst of $IP_3$ in the vicinity of $IP_3$R3s should be relatively short and quickly declining due to depletion of $PIP_2$ in a microvillus, while $IP_3$ continues to diffuse to the cytosol bulk. Moreover, (i) $Ca^{2+}$ store is a very finite $Ca^{2+}$ source so that prolonged $Ca^{2+}$ signaling necessitates $Ca^{2+}$ entry [67]; (ii) $IP_3$Rs are downregulated by released $Ca^{2+}$ [54]. It thus appears that $IP_3$ signaling in type II cells and associated $IP_3$-driven $Ca^{2+}$ release could hardly sustain a high level of intracellular $Ca^{2+}$ required to maintain activity of TRPM5 for sufficiently long time. Meanwhile, DAG turnover is relatively slow [46], and DAG diffusion might be restricted to the microvillus membrane [31]. Hence, potentially, DAG-gated $Ca^{2+}$ entry is capable of prolonging tastant-induced $Ca^{2+}$ signals and sustain TRPM5 activity. In addition, $Ca^{2+}$ entry through store-operated channels (SOCE), which is usually initiated by $Ca^{2+}$ store depletion and provides its recovery [67], also could contribute to a taste-related $Ca^{2+}$ signal [52] (Fig. 8).

To summarize, we speculate here that during taste transduction $IP_3$-driven $Ca^{2+}$ release forms the initial and transient $Ca^{2+}$ signal, which provides the rapid activation of TRPM5 and forms the primary phase of receptor potential. The DAG-regulated $Ca^{2+}$ entry through TRPC3, possibly in concert with SOCE, prolongs the $Ca^{2+}$ signal to preserve TRPM5 activity, thus determining a duration of receptor potential. Further experiments are required to verify this concept, including the assay of TRPC3-deficient mice.

**Supplementary Information** The online version contains supplementary material available at https://doi.org/10.1007/s00424-023-02834-8.

**Author contribution** AC performed electrophysiological and imaging experiments, AK and OR assayed ATP release, MB and NK performed the expression analysis and immunostaining, and SK designed the research and wrote the paper. All authors contributed to data analysis and figure design and reviewed the manuscript.

**Funding** This work was partly supported by the Russian Science Foundation (grant 22-14-00031 to SK).

**Data availability** Not applicable.

## Declarations

**Ethics approval** All experimental protocols were in accordance with local regulatory requirements and the European Communities Council Directive (2010/63/EU) and approved by the Commission on Biosafety and Bioethics (Institute of Cell Biophysics–Pushchino Scientific Center for Biological Research of the Russian Academy of Sciences, Permission no. 4/062020 (June 12, 2020).

**Competing interests** The authors declare no competing interests.

## References

1. Adler E, Hoon MA, Mueller KL, Chandrashekar J, Ryba NJ, Zuker CS (2000) A novel family of mammalian taste receptors. Cell 100:693–702. https://doi.org/10.1016/s0092-8674(00)80705-9
2. Ahmad R, Dalziel JE (2020) G protein-coupled receptors in taste physiology and pharmacology. Front Pharmacol 11:587664. https://doi.org/10.3389/fphar.2020.587664
3. Bakalyar HA, Reed RR (1990) Identification of a specialized adenylyl cyclase that may mediate odorant detection. Science 250:1403–1406. https://doi.org/10.1126/science.2255909
4. Banik DD, Benfey ED, Martin LE, Kay KE, Loney GC, Nelson AR, Ahart ZC, Kemp BT, Kemp BR, Torregrossa A, Medler KF (2020) A subset of broadly responsive type III taste cells contribute to the detection of bitter, sweet and umami stimuli. PLoS Genet 16:e1008925. https://doi.org/10.1371/journal.pgen.1008925
5. Banik DD, Martin LE, Freichel M, Torregrossa AM, Medler KF (2018) TRPM4 and TRPM5 are both required for normal signaling in taste receptor cells. Proc Natl Acad Sci U S A 115:E772–E781. https://doi.org/10.1073/pnas.1718802115
6. Baryshnikov SG, Rogachevskaja OA, Kolesnikov SS (2003) Calcium signaling mediated by P2Y receptors in mouse taste cells. J Neurophysiol 90:3283–3294. https://doi.org/10.1371/journal.pgen.1008925
7. Beech DJ (2012) Integration of transient receptor potential canonical channels with lipids. Acta Physiol (Oxf) 204:227–237. https://doi.org/10.1111/j.1748-1716.2011.02311.x
8. Berridge MJ (2016) The inositol trisphosphate/calcium signaling pathway in health and disease. Physiol Rev 96:1261–1296. https://doi.org/10.1152/physrev.00006.2016
9. Brown JW, McKnight CJ (2010) Molecular model of the microvillar cytoskeleton and organization of the brush border. PLoS ONE 5:e9406. https://doi.org/10.1371/journal.pone.0009406
10. Bystrova MF, Romanov RA, Rogachevskaja OA, Churbanov GD, Kolesnikov SS (2010) Functional expression of the extracellular-$Ca^{2+}$-sensing receptor in mouse taste cells. J Cell Sci 123:972–982. https://doi.org/10.1242/jcs.061879
11. Caicedo A, Jafri MS, Roper SD (2000) In situ $Ca^{2+}$ imaging reveals neurotransmitter receptors for glutamate in taste receptor cells. J Neurosci 20:7978–7985. https://doi.org/10.1523/JNEUROSCI.20-21-07978.2000
12. Caicedo A, Kim KN, Roper SD (2002) Individual mouse taste cells respond to multiple chemical stimuli. J Physiol 544:501–509. https://doi.org/10.1113/jphysiol.2002.027862
13. Caicedo A, Roper SD (2001) Taste receptor cells that discriminate between bitter stimuli. Science 291:1557–1560. https://doi.org/10.1126/science.1056670
14. Chandrashekar J, Mueller KL, Hoon MA, Adler E, Feng L, Guo W, Zuker CS, Ryba NJ (2000) T2Rs function as bitter taste receptors. Cell 100:703–711. https://doi.org/10.1016/s0092-8674(00)80706-0
15. Chandrashekar J, Yarmolinsky D, von Buchholtz L, Oka Y, Sly W, Ryba NJ, Zuker CS (2009) The taste of carbonation. Science 326:443–445. https://doi.org/10.1126/science.1174601
16. Clapp TR, Trubey KR, Vandenbeuch A, Stone LM, Margolskee RF, Chaudhari N, Kinnamon SC (2008) Tonic activity of Galpha-gustducin regulates taste cell responsivity. FEBS Lett 582:3783–3787. https://doi.org/10.1016/j.febslet.2008.10.007

17. Dibattista M, Pifferi S, Boccaccio A, Menini A, Reisert J (2017) The long tale of the calcium activated Cl- channels in olfactory transduction. Channels (Austin) 11:399–414. https://doi.org/10.1080/19336950.2017.1307489
18. Dickson EJ, Falkenburger BH, Hille B (2013) Quantitative properties and receptor reserve of the $IP_3$ and calcium branch of $G_q$-coupled receptor signaling. J Gen Physiol 141:521–535. https://doi.org/10.1085/jgp.201210886
19. Dickson EJ, Hille B (2019) Understanding phosphoinositides: rare, dynamic, and essential membrane phospholipids. Biochem J 476:1–23. https://doi.org/10.1042/BCJ20180022
20. Eichmann TO, Lass A (2015) DAG tales: the multiple faces of diacylglycerol--stereochemistry, metabolism, and signaling. Cell Mol Life Sci 72:3931–3952. https://doi.org/10.1007/s00018-015-1982-3
21. Falkenburger B, Jensen J, Hille B (2010) Kinetics of PIP2 metabolism and KCNQ2/3 channel regulation studied with a voltage-sensitive phosphatase in living cells. J Gen Physiol 135:99–114. https://doi.org/10.1085/jgp.200910345
22. Fesenko EE, Kolesnikov SS, Lyubarsky AL (1985) Induction by cyclic GMP of cationic conductance in plasma membrane of retinal rod outer segment. Nature 313:310–313. https://doi.org/10.1038/313310a0
23. Fettiplace R, Kim KX (2014) The physiology of mechanoelectrical transduction channels in hearing. Physiol Rev 94:951–986. https://doi.org/10.1152/physrev.00038.2013
24. Gillespie PG, Müller U (2009) Mechanotransduction by hair cells: models, molecules, and mechanisms. Cell 139:33–44. https://doi.org/10.1016/j.cell.2009.09.010
25. Hacker K, Laskowski A, Feng L, Restrepo D, Medler K (2008) Evidence for two populations of bitter responsive taste cells in mice. J Neurophysiol 99:1503–1514. https://doi.org/10.1152/jn.00892.2007
26. Hashimotodani Y, Ohno-Shosaku T, Tsubokawa H, Ogata H, Emoto K, Maejima T, Araishi K, Shin HS, Kano M (2005) Phospholipase Cbeta serves as a coincidence detector through its $Ca^{2+}$ dependency for triggering retrograde endocannabinoid signal. Neuron 45:257–268. https://doi.org/10.1016/j.neuron.2005.01.004
27. Hisatsune C, Yasumatsu K, Takahashi-Iwanaga H, Ogawa N, Kuroda Y, Yoshida R, Ninomiya Y, Mikoshiba K (2007) Abnormal taste perception in mice lacking the type 3 inositol 1,4,5-trisphosphate receptor. J Biol Chem 282:37225–37231. https://doi.org/10.1074/jbc.M705641200
28. Horowitz LF, Hirdes W, Byung-Chang S, Hilgemann D, Mackie K, Hille B (2005) Phospholipase C in living cells: activation, inhibition, $Ca^{2+}$ requirement, and regulation of M current. J Gen Physiol 126:243–262. https://doi.org/10.1085/jgp.200509309
29. Kinnamon SC (2016) G protein–coupled taste transduction. In: Zufall F, Munger SD (eds) Chemosensory Transduction, 1st edn. Elsevier, New York, pp 271–285
30. Kolesnikov SS, Margolskee RF (1998) Extracellular $K^+$ activates a $K^+$- and $H^+$-permeable conductance in frog taste cells. J Physiol 507:415–432. https://doi.org/10.1111/j.1469-7793.1998.415bt.x
31. Lange K (2011) Fundamental role of microvilli in the main functions of differentiated cells: outline of an universal regulating and signaling system at the cell periphery. J Cell Physiol 226:896–927. https://doi.org/10.1002/jcp.22302
32. Leinders-Zufall T, Rand MN, Shepherd GM, Greer CA, Zufall F (1997) Calcium entry through cyclic nucleotide-gated channels in individual cilia of olfactory receptor cells: spatiotemporal dynamics. J Neurosci 17:4136–4148. https://doi.org/10.1523/JNEUROSCI.17-11-04136.1997
33. Lewandowski BC, Sukumaran SK, Margolskee RF, Bachmanov AA (2016) Amiloride-insensitive salt taste is mediated by two populations of type III taste cells with distinct transduction mechanisms. J Neurosci 36:1942–1953. https://doi.org/10.1523/JNEUROSCI.2947-15.2016
34. Lievremont JP, Bird GS, Putney JW Jr (2005) Mechanism of inhibition of TRPC cation channels by 2-aminoethoxydiphenylborane. Mol Pharmacol 68:758–762. https://doi.org/10.1124/mol.105.012856
35. Liman ER, Corey DP, Dulac C (1999) TRP2: a candidate transduction channel for mammalian pheromone sensory signaling. Proc Natl Acad Sci U S A 96:5791–5796. https://doi.org/10.1073/pnas.96.10.5791
36. Liman ER, Kinnamon SC (2021) Sour taste: receptors, cells and circuits. Curr Opin Physiol 20:8–15. https://doi.org/10.1016/j.cophys.2020.12.006
37. Lindemann B (1996) Taste reception. Physiol Rev 76:719–766. https://doi.org/10.1152/physrev.1996.76.3.719
38. Lindemann B (2001) Receptors and transduction in taste. Nature 413:219–225. https://doi.org/10.1038/35093032
39. Lucas P, Ukhanov K, Leinders-Zufall T, Zufall F (2003) A diacylglycerol-gated cation channel in vomeronasal neuron dendrites is impaired in TRPC2 mutant mice: mechanism of pheromone transduction. Neuron 40:551e561. https://doi.org/10.1016/s0896-6273(03)00675-5
40. Lumpkin EA, Marquis RE, Hudspeth AJ (1997) The selectivity of the hair cell's mechanoelectrical-transduction channel promotes $Ca^{2+}$ flux at low $Ca^{2+}$ concentrations. Proc Natl Acad Sci U S A 94:10997–11002. https://doi.org/10.1073/pnas.94.20.10997
41. Ma Z, Taruno A, Ohmoto M, Jyotaki M, Lim JC, Miyazaki H, Niisato N, Marunaka Y, Lee RJ, Hoff H, Payne R, Demuro A, Parker I, Mitchell CH, Henao-Mejia J, Tanis JE, Matsumoto I, Tordoff MG, Foskett JK (2018) CALHM3 is essential for rapid ion channel-mediated purinergic neurotransmission of GPCR-mediated tastes. Neuron 98:547–561.e10. https://doi.org/10.1016/j.neuron.2018.03.043
42. Medler KF (2015) Calcium signaling in taste cells. Biochim Biophys Acta 1853:2025–2032. https://doi.org/10.1016/j.bbamcr.2014.11.013
43. Menco BP, Carr VM, Ezeh PI, Liman ER, Yankova MP (2001) Ultrastructural localization of G-proteins and the channel protein TRP2 to microvilli of rat vomeronasal receptor cells. J Comp Neurol 438:468–489. https://doi.org/10.1002/cne.1329
44. Murray RG (1973) The ultrastructure of taste buds. In: Friedmann I (ed) The ultrastructure of sensory organs. North Holland Pub Co, Amsterdam, pp 1–81
45. Murtaza B, Hichami A, Khan AS, Plesnik J, Sery O, Dietrich A, Birnbaumer L, Khan NA (2021) Implication of TRPC3 channel in gustatory perception of dietary lipids. Acta Physiol (Oxf) 231:e13554. https://doi.org/10.1111/apha.13554
46. Myeong J, de la Cruz L, Jung SR, Yeon JH, Suh BC, Koh DS, Hille B (2020) Phosphatidylinositol 4,5-bisphosphate is regenerated by speeding of the PI 4-kinase pathway during long PLC activation. J Gen Physiol 152:e202012627. https://doi.org/10.1085/jgp.202012627
47. Nakamura T, Gold GH (1987) A cyclic nucleotide-gated conductance in olfactory receptor cilia. Nature 325:442–444. https://doi.org/10.1038/325442a0
48. Nelson G, Chandrashekar J, Hoon MA, Feng L, Zhao G, Ryba NJ, Zuker CS (2002) An amino-acid taste receptor. Nature 416:199–202. https://doi.org/10.1038/nature726
49. Nelson G, Hoon MA, Chandrashekar J, Zhang Y, Ryba NJ, Zuker CS (2001) Mammalian sweet taste receptors. Cell 106:381–390. https://doi.org/10.1016/s0092-8674(01)00451-2
50. Nilius B (2003) Calcium-impermeable monovalent cation channels: a TRP connection? Br J Pharmacol 138:5–7. https://doi.org/10.1038/sj.bjp.0705073

51. Nomura K, Nakanishi M, Ishidate F, Iwata K, Taruno A (2020) All-electrical $Ca^{2+}$-independent signal transduction mediates attractive sodium taste in taste buds. Neuron 106:816–829. https://doi.org/10.1016/j.neuron.2020.03.006
52. Ogura T, Margolskee RF, Kinnamon SC (2002) Taste receptor cell responses to the bitter stimulus denatonium involve $Ca^{2+}$ influx via store-operated channels. J Neurophysiol 87:3152–3155. https://doi.org/10.1152/jn.2002.87.6.3152
53. Oka Y, Butnaru M, von Buchholtz L, Ryba NJ, Zuker CS (2013) High salt recruits aversive taste pathways. Nature 494:472–475. https://doi.org/10.1038/nature11905
54. Parys JB, Vervliet T (2020) New insights in the IP3 receptor and its regulation. Adv Exp Med Biol 1131:243–270. https://doi.org/10.1007/978-3-030-12457-1_10
55. Perez CA, Margolskee RF, Kinnamon SC, Ogura T (2003) Making sense with TRP channels: store-operated calcium entry and the ion channel Trpm5 in taste receptor cells. Cell Calcium 33:541–549. https://doi.org/10.1016/s0143-4160(03)00059-9
56. Prole DL, Taylor CW (2019) Structure and function of IP3 receptors. Cold Spring Harb Perspect Biol 11:a035063. https://doi.org/10.1101/cshperspect.a035063
57. Roebber JK, Roper SD, Chaudhari N (2019) The role of the anion in salt (NaCl) detection by mouse taste buds. J Neurosci 39:6224–6232. https://doi.org/10.1523/JNEUROSCI.2367-18.2019
58. Romanov RA, Kolesnikov SS (2006) Electrophysiologically identified subpopulations of taste bud cells. Neurosci Lett 395:249–254. https://doi.org/10.1016/j.neulet.2005.10.085
59. Romanov RA, Lasher RS, High B, Savidge LE, Lawson A, Rogachevskaja OA, Zhao H, Rogachevsky VV, Bystrova MF, Churbanov GD, Adameyko I, Harkany T, Yang R, Kidd GJ, Marambaud P, Kinnamon JC, Kolesnikov SS, Finger TE (2018) Chemical synapses without synaptic vesicles: purinergic neurotransmission through a CALHM1 channel-mitochondrial signaling complex. Sci Signal 11:eaao1815. https://doi.org/10.1126/scisignal.aao1815
60. Romanov RA, Rogachevskaja OA, Bystrova MF, Jiang P, Margolskee RF, Kolesnikov SS (2007) Afferent neurotransmission mediated by hemichannels in mammalian taste cells. EMBO J 26:657–667. https://doi.org/10.1038/sj.emboj.7601526
61. Roper SD, Chaudhari N (2017) Taste buds: cells, signals and synapses. Nat Rev Neurosci 18:485–497. https://doi.org/10.1038/nrn.2017.68
62. Schleifer H, Doleschal B, Lichtenegger M, Oppenrieder R, Derler I, Frischauf I, Glasnov TN, Kappe CO, Romanin C, Groschner K (2012) Novel pyrazole compounds for pharmacological discrimination between receptor-operated and store-operated $Ca^{2+}$ entry pathways. Br J Pharmacol 167:1712–1722. https://doi.org/10.1111/j.1476-5381.2012.02126.x
63. Spehr M (2016) Vomeronasal transduction and cell signaling. In: Zufall F, Munger SD (eds) Chemosensory transduction. The detection of odors, tastes, and other chemostimuli, 1st edn. Academic Press, pp 191–206
64. Svobodova B, Groschner K (2016) Mechanisms of lipid regulation and lipid gating in TRPC channels. Cell Calcium 59:271–279. https://doi.org/10.1016/j.ceca.2016.03.012
65. Taruno A, Nomura K, Kusakizako T, Ma Z, Nureki O, Foskett JK (2021) Taste transduction and channel synapses in taste buds. Pflugers Arch 473:3–13. https://doi.org/10.1007/s00424-020-02464-4
66. Taruno A, Vingtdeux V, Ohmoto M, Ma Z, Dvoryanchikov G, Li A, Adrien L, Zhao H, Leung S, Abernethy M, Koppel J, Davies P, Civan MM, Chaudhari N, Matsumoto I, Hellekant G, Tordoff MG, Marambaud P, Foskett JK (2013) CALHM1 ion channel mediates purinergic neurotransmission of sweet, bitter and umami tastes. Nature 495:223–226. https://doi.org/10.1038/nature11906
67. Thillaiappan NB, Chakraborty P, Hasan G, Taylor CW (2019) IP3 receptors and $Ca^{2+}$ entry. Biochim Biophys Acta Mol Cell Res 1866:1092–1100. https://doi.org/10.1016/j.bbamcr.2018.11.007
68. Tu YH, Cooper AJ, Teng B, Chang RB, Artiga DJ, Turner HN, Mulhall EM, Ye W, Smith AD, Liman ER (2018) An evolutionarily conserved gene family encodes proton-selective ion channels. Science 359:1047–1050. https://doi.org/10.1126/science.aao3264
69. Wellendorph P, Bräuner-Osborne H (2009) Molecular basis for amino acid sensing by family C G-protein-coupled receptors. Br J Pharmacol 156:869–884. https://doi.org/10.1111/j.1476-5381.2008.00078.x
70. Wilson CE, Lasher RS, Yang R, Dzowo Y, Kinnamon JC, Finger TE (2022) Taste bud connectome: implications for taste information processing. J Neurosci 42:804–816. https://doi.org/10.1523/jneurosci.0838-21.2021
71. Xu X, Lozinskaya I, Costell M, Lin Z, Ball JA, Bernard R, Behm DJ, Marino JP, Schnackenberg CG (2013) Characterization of small molecule TRPC3 and TRPC6 agonist and antagonists. Biophys J 104:454a. https://doi.org/10.1016/j.bpj.2012.11.2513
72. Yang R, Dzowo YK, Wilson CE, Russell RL, Kidd GJ, Salcedo E, Lasher RS, Kinnamon JC, Finger TE (2020) Three-dimensional reconstructions of mouse circumvallate taste buds using serial blockface scanning electron microscopy: I. Cell types and the apical region of the taste bud. J Comp Neurol 528:756–771. https://doi.org/10.1002/cne.24779
73. Yau KW, Hardie RC (2009) Phototransduction motifs and variations. Cell 139:246–264. https://doi.org/10.1016/j.cell.2009.09.029
74. Zhang Y, Hoon MA, Chandrashekar J, Mueller KL, Cook B, Wu D, Zuker CS, Ryba NJ (2003) Coding of sweet, bitter, and umami tastes: different receptor cells sharing similar signaling pathways. Cell 112:293–301. https://doi.org/10.1016/s0092-8674(03)00071-0
75. Zufall F, Leinders-Zufall T (2000) The cellular and molecular basis of odor adaptation. Chem Senses 25:473–481. https://doi.org/10.1093/chemse/25.4.473


**Publisher's note** Springer Nature remains neutral with regard to jurisdictional claims in published maps and institutional affiliations.

Springer Nature or its licensor (e.g. a society or other partner) holds exclusive rights to this article under a publishing agreement with the author(s) or other rightsholder(s); author self-archiving of the accepted manuscript version of this article is solely governed by the terms of such publishing agreement and applicable law.